THE ASTROPHYSICAL JOURNAL, 229: 1–13, 1979 April 1

THE INFRARED LUMINOSITY/H I VELOCITY-WIDTH RELATION AND ITS APPLICATION TO THE DISTANCE SCALE

MARC AARONSON*
Steward Observatory, University of Arizona

JOHN HUCHRA*
Harvard-Smithsonian Center for Astrophysics

AND

JEREMY MOULD
Kitt Peak National Observatory†
Received 1978 July 6; accepted 1978 October 3

ABSTRACT

The Tully-Fisher relation between the luminosity of late-type galaxies and their global 21 cm velocity widths has been investigated with infrared photometry. Multiaperture magnitudes at H(1.6 μm) have been obtained for 11 spiral galaxies in Virgo and 18 in the Ursa Major cluster. A tighter empirical correlation between luminosity and 21 cm line width has been found for H magnitudes *uncorrected for inclination* than for photographic magnitudes with their individually uncertain, prescribed corrections for internal absorption. The similarity of the infrared magnitude/velocity-width correlation for Virgo, for Ursa Major, and for six nearby galaxies also measured suggests that the slope of the relationship is universal in nature.

An important uncertainty in previous applications of the Tully-Fisher method was an incomplete understanding of its physical basis. In the infrared the slope of the magnitude/velocity-width relation is found to be considerably steeper than that obtained optically. From this result, we demonstrate that the dynamical origin of the relationship is similar to the well-known $L \propto V^4$ power law for elliptical galaxies. We further suggest that this has not been seen in the blue, because the mass-to-luminosity ratio M/L_B varies markedly in spirals of differing mass, whereas M/L_H is more nearly constant.

By using a provisional calibration based on the distances of Sandage and Tammann for local galaxies, we derive distance moduli to Virgo and Ursa Major of 31.07 ± 0.20 and 31.08 ± 0.16. A mean value for the Hubble constant of $H_0 = 61 \pm 4$ km s^{-1} Mpc^{-1} follows from these preliminary results.

We believe that the infrared magnitude/velocity-width relation is now the most powerful tool available for determining redshift-independent distances to the adjacent great clusters.

Subject headings: cosmology — galaxies: clusters of — infrared: general — radio sources: 21 cm radiation

I. INTRODUCTION

The relationship discovered by Tully and Fisher (1977, hereafter TF) between absolute blue magnitudes and H I profile widths of galaxies provides a luminosity calibration to substantial distances. Like other tertiary distance indicators involving the global properties of galaxies, however, the Tully-Fisher relation requires a number of significant corrections to the observables, which are more or less uncertain because of the diverse characteristics of late-type spirals. The most important of these, according to Sandage and Tammann (1976*b*, hereafter ST), is the correction for internal absorption to the blue magnitudes, which may exceed 1.0 mag for highly inclined objects. Although statistically a simple function of inclination, this correction probably has a large random component. A second correction is required to convert the measured 21 cm profile width (ΔV) to an edge-on value, where it becomes a measure of the maximum rotation velocity ($V_{\rm max}$) in disk galaxies. A third correction is for the galactic extinction in the observed direction. Another uncertainty in the relationship is the amount of scatter introduced by the wide range of morphological types. A final uncertainty in the application of the Tully-Fisher relation is the inability to understand its physical basis beyond the general idea that $V_{\rm max}$ must measure mass and hence luminosity. The vagueness of the physics raises the specter of nonlinearity or discontinuity in the relationship.

Since extinction corrections of the size discussed above virtually disappear in the infrared, we have carried out a program (§ III) to measure infrared magnitudes for all the TF galaxies in the Virgo and Ursa

* Guest Investigator at Kitt Peak National Observatory.

† Operated by the Association of Universities for Research in Astronomy, Inc., under contract with the National Science Foundation.

Major clusters. The results confirm the hypothesis that extinction is indeed a major source of scatter in the Tully-Fisher relation. A much tighter relationship is found from the infrared photometry (§ V). Unexpectedly, however, the new photometry also reveals the true form of the relationship to be an $L \propto V^4$ law (§§ VI and VII). Finally (§ VIII), with provisional photometry of the "Local Calibrator" galaxies, we determine the Virgo and Ursa Major distance moduli to obtain a preliminary value of the Hubble constant. In § IX our results are summarized, and uncertainties and future requirements are discussed.

II. DISCUSSION OF PREVIOUS WORK

In this section we briefly review and compare the work of TF and ST. The analyses by these authors differ in a number of important respects. First, different inclination corrections are applied to the magnitudes. Tully and Fisher adopt the simple relation $A_B = 0.28\,(a/b - 1)$; while ST use $A_B = \alpha(a/b)$, where a/b is the axial ratio, and the constant α depends on morphological type. While both procedures are based on the work of Holmberg (1958), note that in the former case galaxies are corrected only to face-on orientation, whereas in the latter the correction is for total internal absorption. Although small, another difference between ST and TF is in the adopted velocity profile widths, with ST generally preferring values from Huchtmeier, Tammann, and Wendker (1976). A third difference lies in the assumed value of inclination. The inclinations adopted by ST are calculated primarily from axial ratios taken from Holmberg (1958) and/or de Vaucouleurs and de Vaucouleurs (1964). Tully and Fisher (1976) and Fisher and Tully (1977) argue that values so determined are subject to systematic errors in the sense of predicting orientations that are too face-on in comparison with inclinations determined from the opening of the spiral arms.[1] In TF the adopted inclinations were, whenever possible, weighted by the optical appearance of the spiral structure. For the eight Virgo galaxies in common between TF, ST, and this paper, only two have inclinations assumed by TF and ST that differ by more than 4°: NGC 4178 ($\Delta = 8°$) and NGC 4651 ($\Delta = 11°$).

The final and perhaps most important difference between TF and ST is in the sample of Virgo galaxies considered. Sandage and Tammann introduce 12 additional Virgo galaxies, nine of which are more face-on than 45°. To some extent this vitiates the entire method, for while the size of the magnitude correction decreases for face-on galaxies, the error in the velocity width (which is corrected to edge-on as csc i) dramatically increases (e.g., see ST's Fig. 2). Furthermore, there is a systematic effect in the data, so that galaxies more face-on give systematically larger distance moduli than those more edge-on (ST; Fisher and Tully 1977). It seems probable to us that this effect is due to a combination of errors in (*a*) the inclination correction to the H I velocity width for galaxies more face-on than 45°, and (*b*) the inclination correction to the magnitudes for galaxies more edge-on than 45°.

Keeping in mind the above differences, TF found distance moduli to Virgo and Ursa Major of 30.8 ± 0.2 mag and 30.7 ± 0.35 mag, respectively, which, assuming these clusters are not significantly perturbed relative to the Hubble flow, lead to Hubble constant values of 76 ± 8 km s^{-1} Mpc^{-1} and 69 ± 11 km s^{-1} Mpc^{-1}. (Following ST, we have adjusted the TF distance moduli to correspond to a revised Hyades modulus [Hanson 1975] of 3.23, which we adopt for the remainder of this paper. Also, our assumed mean redshifts for the two clusters are discussed in § VIII*b*.) Sandage and Tammann, on the other hand, using the Tully-Fisher method, find a distance modulus to Virgo of 31.6 ± 0.2 mag, which leads to a Hubble constant of 53 ± 6 km s^{-1} Mpc^{-1}. They stress that this lower value agrees with and adds support to the similarly low value of 50 ± 4 km s^{-1} Mpc^{-1} obtained by them from several other techniques (ST and references therein). In a more recent analysis, Fisher and Tully (1977) attempt to minimize their differences with ST by accepting the ST Local Calibration (which differs only a little from that used in TF), the ST inclination correction procedure, and, in some but not all cases, the ST velocity profile widths and inclinations. However, they accept only galaxies more edge-on than 45°, and derive a distance modulus to Virgo of 31.0 ± 0.2 mag, which is still 0.6 mag less than the ST value.

Note that all of the above distance moduli are derived from and depend directly upon the distances to the Local Calibrators adopted by ST. However, these distances are not unanimously accepted (e.g., see de Vaucouleurs 1978*a*, *b* and van den Bergh 1976).

III. OBSERVATIONS AND DATA REDUCTION

To obtain infrared magnitudes, we have selected the H band at 1.6 μm. This wavelength has several advantages over the other conventional broad-band windows. First, for large-beam infrared work, the signal-to-noise ratio at H is greatest. Second, stars are virtually the only contributors to the light. In general there is little or no contamination from dust or gaseous emission at H, as might be true at K (2.2 μm; see Aaronson 1979, hereafter Paper V). Finally, at Kitt Peak the extinction per unit air mass at H on a photometric night is typically only 0.04–0.07 mag.

Multiaperture observations at H were obtained for eight galaxies in the Virgo cluster, 18 galaxies in the Ursa Major cluster, and three Local Calibrators during a 4 day run in 1978 May with the KPNO No. 1, 0.9 m telescope. The data are presented in Tables 1–3. Three additional galaxies in Virgo were also observed in 1978 May on the KPNO 2.1 m telescope; data for these are given in the bottom part of Table 1. All of the galaxies observed were taken directly from TF.

[1] For dramatic examples of the two problem cases cited by Fisher and Tully (1977)—(*a*) spiral structure opening onto the minor axis and (*b*) the presence of a pronounced nuclear bulge—see photographs of NGC 4321 and 4594 in Sandage (1961).

TABLE 1

Virgo Cluster Data

Name	Type	log $D(0)$*	H (mag) Ap: 40".6	51".8	82".6	102".2	$H_{-0.5}$ (mag)	$\Delta V(0)$ (km s^{-1})
NGC 4192	SX(s)ab	1.87	—	8.58	8.23	8.06	7.82	465
NGC 4535	SX(s)c	1.80	—	9.72	9.27	8.96	8.74	436:
NGC 4501	SA(rs)b	1.78	—	7.95	7.45	7.24	7.13	592
NGC 4654	SX(rs)cd	1.63	—	9.31	8.78	8.60	8.80	368
NGC 4178	SB(rs)dm	1.61	—	10.57	10.07	9.84	10.14	293
NGC 4206	SA(s)bc:	1.57	—	10.54	10.23	—	10.34	301
NGC 4651	SA(rs)c	1.54	9.09	8.82	8.49	8.38	8.66	440
IC 769	SA bc	1.36	11.53±0.05	11.21±0.04	—	—	11.44	323
			Ap: 23".1	44".4				
NGC 4498	SX(s)cd	1.45	11.74	10.98	—	—	10.77	214
NGC 4532	IBm	1.37	11.31	10.45	—	—	10.45	294:
NGC 4758	SBb?	1.37	11.90	11.23	—	—	11.23	213

*$D(0)$ in units of 0.1 minutes.

The entire set of galaxy observations was measured with the Harvard-Smithsonian InSb detector system; a focal-plane chopper and offset guider were always employed. The H filter had a central wavelength and a bandwidth of 1.65 μm and 0.30 μm, respectively, and was cooled to pumped nitrogen temperature. Unless otherwise noted in the tables, the photometric uncertainty of the data was always $\lesssim$0.03 mag. The true accuracy was probably limited more by centering errors than by statistical errors (which were typically $<$0.02 mag) or by the photometric quality of the nights (which was always $\sim$0.01 mag). Most of the objects observed were edge-on spirals, and a well-defined nucleus was often absent. In these cases the signal was "peaked up" by scans through the galaxy. In all but one instance (NGC 3556, see below) there was clear correspondence between the infrared peak and the center of the overall visual luminosity distribution. Because of weak signal strength, the faintest galaxies in Virgo and Ursa Major could only be centered visually. While time allowed for repetition of only three galaxy measurements (including the two faintest Ursa Major objects), the agreement between the repeated observations was excellent. The system of standard stars to which the data are referred is discussed fully in Frogel *et al.* (1978); in this system $H(\alpha$ Lyr$)$ = 0.0 mag.

Chopping was usually in the north-south direction.

TABLE 2

Ursa Major Cluster Data

Name	Type	log $D(0)$	H (mag) Ap: 40".6	51".8	82".6	102".2	$H_{-0.5}$ (mag)	$\Delta V(0)$ (km s^{-1})
NGC 3992	SB(rs)bc	1.83	—	8.89	8.48	8.27	8.04	558
NGC 3556	SB(s)cd	1.80	—	9.10	8.47	8.26	8.11	340
NGC 3953	SB(r)bc	1.76	—	8.66	8.20	8.02	7.97	483
NGC 4157	SAB(s)b?	1.69	—	8.84	8.43	8.30	8.35	431
NGC 4088	SAB(rs)bc	1.67	—	9.06	8.52	8.33	8.46	407
NGC 4217	Sb	1.63	—	9.09	8.65	—	8.67	427
NGC 4100	SA(rs)bc	1.62	—	9.32	8.84	8.64	8.88	412
NGC 3877	SA(s)c:	1.60	—	9.02	8.64	8.53	8.71	346
NGC 3893	SAB(rs)c:	1.59	—	9.07	8.71	8.51	8.80	370
NGC 4013	Sb	1.57	9.02	8.76	8.45	8.35	8.56	406
NGC 3917	SAcd:	1.57	—	10.48	9.91	9.69	10.11	283
UGC 6983	SB(rs)cd	1.55	—	11.91±0.06	11.48±0.06	—	11.67	287:
NGC 4183	SA(s)cd?	1.53	11.16±0.06	10.92±0.05	—	—	10.72	253
NGC 3972	SA(s)bc	1.49	10.88	10.63	10.11	—	10.50	270
NGC 4010	SB(s)cd:	1.47	10.82±0.04	10.56	—	—	10.49	283
UGC 7089	Sdm-m	1.43	12.30±0.04	11.91±0.05	—	—	11.95	160
UGC 6399	Sm	1.40	12.46±0.07	12.37±0.05	—	—	12.40	175
NGC 4085	SAB(s)c:	1.34	10.08	9.94	9.67	—	10.07	310

TABLE 3

DATA FOR LOCAL CALIBRATORS

	NGC 5585	NGC 5204	Ho IV
Type	SAB(s)d	SA(s)m	SB(s)m
log $D(0)$	1.70	1.63	1.49
H (mag)			
Ap: 40″6	-	-	13.35±0.11
51″8	10.85	10.91±0.04	12.92±0.12
82″6	10.30	10.34	-
102″2	10.10±0.04	10.12±0.04	-
$H_{-0.5}$ (mag)	10.16	10.37	12.73
$\Delta V(0)$ (km s^{-1})	214	151	110
d (Mpc)	7.94	7.94	7.94
$H_{-0.5}^{abs}$	-19.34	-19.13	-16.77

The chopper throws used were 168″ on the 0.9 m and 75″ on the 2.1 m. Palomar Sky Survey prints were checked for the presence of stars in the "reference" beam. If any were present, the measurement was made either "single beam" or by rotating the photometer away from north-south alignment.

In order to stress the power and simplicity of using H magnitudes, the data in Tables 1–3 were corrected for atmospheric extinction only. No correction was applied for internal absorption due to galaxian inclination, interstellar absorption in our own Galaxy, or redshift effect. Since $A_H/A_B \approx 0.1$ according to van de Hulst curve No. 15 (Johnson 1968), and $K_H \approx 0.35\,z$ (Frogel *et al.* 1978), the size of those corrections is typically <0.1, <0.01, and <0.01 mag, respectively. Note that the appropriate inclination correction is both poorly determined and controversial (see § II), so the uncertainty in any correction that might be applied at H is probably as big as the correction itself. No correction was applied for extended galaxian flux in the reference beam, but the chopping throws were long enough so that any such correction would be <0.01 mag. Finally, the beam profiles were sufficiently flat that any magnitude correction of the type discussed by Frogel *et al.* (1978) would be <0.02 mag and has thus been ignored.

In order to correct the H magnitudes to the same isophotal aperture size, we chose a visually determined diameter system, as the required surface photometry in the infrared is nonexistent. We selected the D system used by de Vaucouleurs, de Vaucouleurs, and Corwin (1976) in the *Second Reference Catalogue of Bright Galaxies* (hereafter RC2). Except in three cases, the morphological types and log $D(0)$ values listed in Tables 1–3 have been taken directly from RC2. Three galaxies (IC 769 in Virgo; UGC 7089 and 6399 in Ursa Major) are not listed in RC2. For these objects types and diameters were obtained from Nilson (1973, hereafter UGC). A comparison was first made between the diameters listed in RC2 and those transformed from the UGC to the $D(0)$ system by using the equations given in RC2. For 10 Virgo galaxies, the difference $\Delta = \log D(0) - \log D(0)_{\rm UGC}$ was found to be 0.005 with a dispersion of 0.04. For 16 Ursa Major galaxies, the result was $\Delta = 0.02 \pm 0.02$. Thus the log $D(0)$ value adopted for IC 769 was simply the transformed UGC value, while for UGC 7089 and 6399, 0.02 was added to the transformed UGC values.

Listed in Tables 1–3 are H magnitudes at $\log A/D(0) = -0.5$ (hereafter $H_{-0.5}$). The value -0.5 was chosen as a compromise between maximizing the aperture size and minimizing the amount of extrapolation required. The $H_{-0.5}$ magnitudes listed in Tables 1–3 were found by simple interpolation or extrapolation in the $[H, \log A/D(0)]$-plane. Over the limited aperture ranges involved, the growth curves in this plane are virtually straight lines.

The $D(0)$ values we have used are corrected for inclination (see RC2) but not for extinction in our own Galaxy, as the latter is both very small and somewhat uncertain. We also investigated the use of H magnitudes at $\log A/D = -0.6$ (i.e., diameters uncorrected for inclination), which in the mean are roughly equal to H at $\log A/D(0) = -0.5$. Neither the scatter of points nor the correlations discussed below differed significantly. We estimate that the uncertainty in the diameters is $\lesssim 5\%$, which leads to a typical error in $H_{-0.5} \lesssim 0.05$ mag.

In Tables 1–3 we also list 21 cm velocity profile widths taken directly from TF.

IV. THE LOCAL CALIBRATORS PROBLEM

In order to obtain absolute distances, and thus an estimate of the Hubble constant, a calibration of the magnitude/velocity-width relation is needed for galaxies whose distances are known from independent methods (e.g., sizes of H II regions, brightest stars, etc.). We are then limited to nearby galaxies with rather large projected diameters—for the seven additional Local Calibrators used by TF, the apertures required for $H_{-0.5}$ range from 120″ up to 2700″. However, for early-type spirals, the problem is not as intractable as it might sound, because the H growth curves for such galaxies are in general extremely well behaved.

In Figure 1 we have plotted the H growth curves for three subsets of galaxies: types S0/a, Sa, Sab (nine objects); types Sb, Sbc (28 objects); and types Sc, Scd, Sd (16 objects). The data used to construct

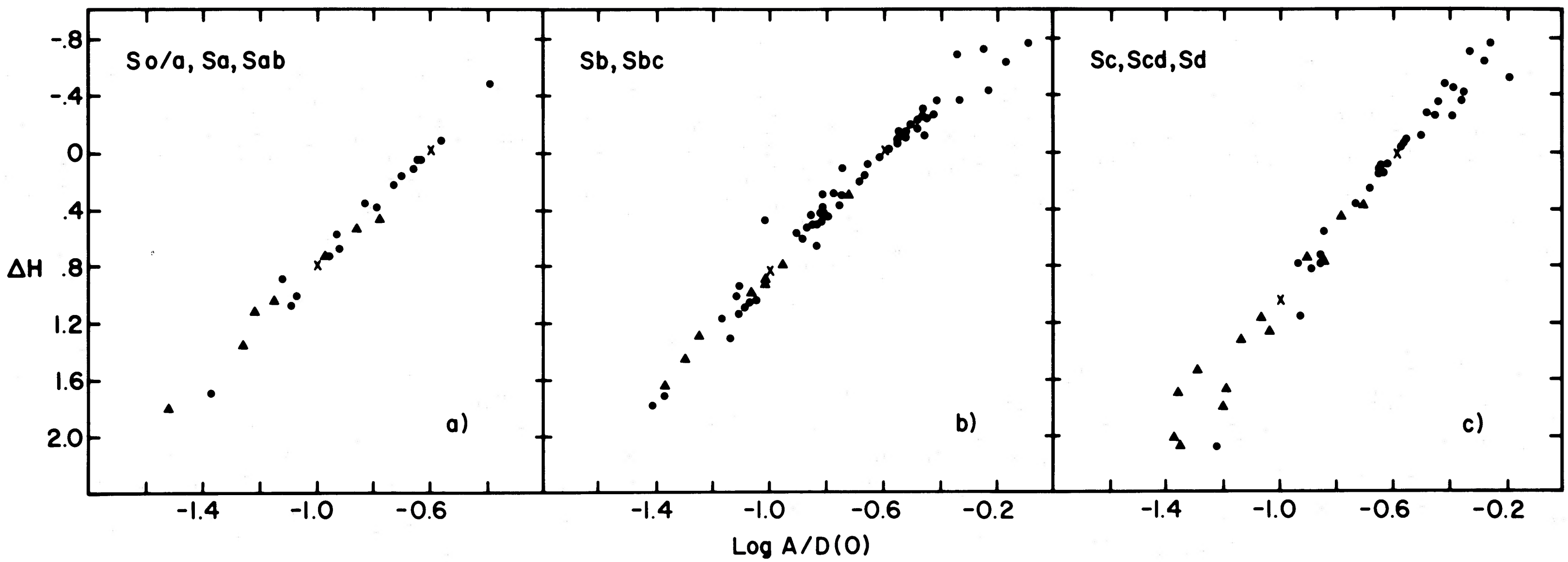

FIG. 1.—The growth curve at H is plotted for three subsets of galaxies. *Crosses*, normalization points, not data. The filled circles have been normalized to the crosses at $\log A/D(0) = -0.6$, while the triangles have been normalized to the crosses at $\log A/D(0) = -1.0$.

TABLE 4

DATA FOR ADDITIONAL LOCAL CALIBRATORS

Name	Type	log $D(0)$	log $A/D(0)$	H (mag)	$H_{-0.5}$ (mag)	$\Delta V(0)$ (km s^{-1})	d (Mpc)	$H_{-0.5}^{\rm abs}$
NGC 224	SA(s)b	3.15	-2.49	6.04				
			-2.20	4.93				
			-1.90	3.94	0.79	546	0.731	-23.53
NGC 3031	SA(s)ab	2.35	-1.81	7.06				
			-1.57	6.42				
			-1.51	6.34				
			-1.10	5.43	4.23	530	3.56	-23.53
NGC 2403	SAB(s)cd	2.20	-0.96	7.85±0.05	6.70	306	3.56	-21.06

Figure 1 were obtained from Tables 1–3 and from Paper V. Data for all nonpeculiar galaxies that range in type from S0/a to Sd and that have multiaperture measurements were used.

Suitable H magnitudes for three additional Local Calibrators obtained with the same instrumental setup discussed above are available from Paper V. These are summarized in Table 4. The values of $H_{-0.5}$ given for NGC 2403 and 3031 were obtained by extrapolation along the growth curves in Figures 1*c* and 1*a*, respectively. For NGC 224 (M31), a three-part extrapolation was required. From a log $A/D(0)$ of -1.90 to -1.81, we used the M31 H growth curve; from -1.81 to -1.10, the NGC 3031 H growth curve was used; and from -1.10 to -0.5, we used the H growth curve in Figure 1*b*. The types and log $D(0)$ values in Table 4 are again from RC2, and the $\Delta V(0)$ values are from TF.

We stress that although extrapolation is not the most desirable approach for effecting a calibration, the procedure followed here is not a blind one. The growth curves employed are rather well established; they exhibit a scatter in ΔH of only ~0.10 mag in the range -1.0 to -0.5 in log $A/D(0)$, implying that the uncertainty in our estimated $H_{-0.5}$ magnitudes for NGC 2403 and 3031 is of a similar value. This is as

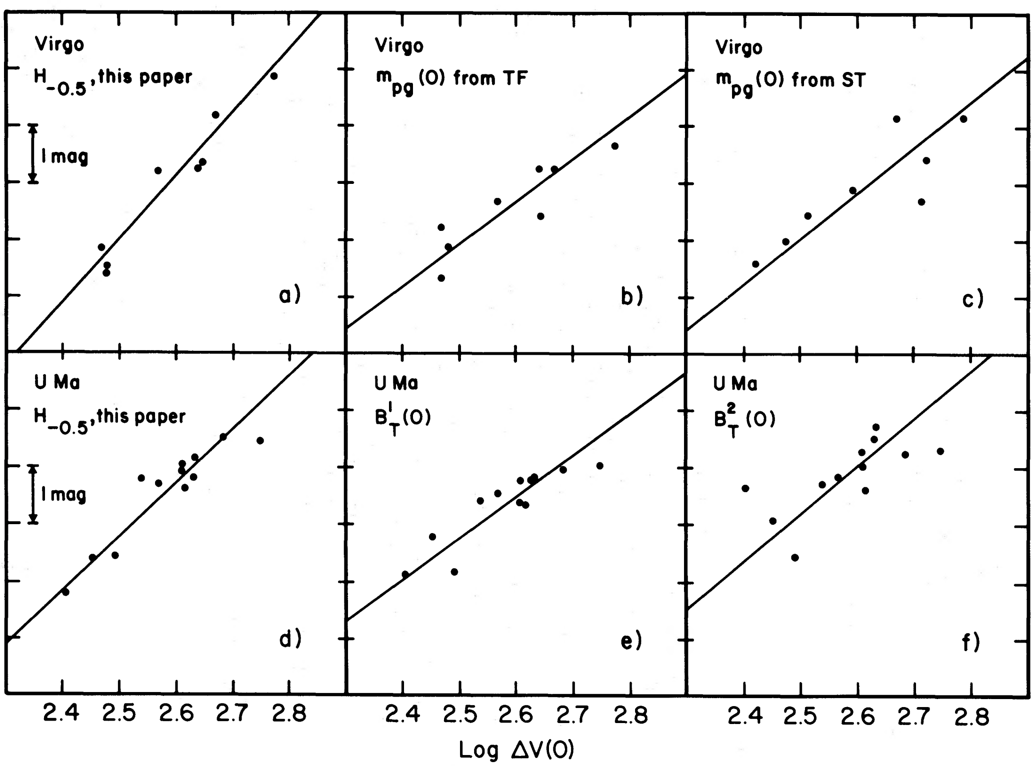

FIG. 2.—Various magnitudes are plotted against log $\Delta V(0)$. Least-squares solutions are also shown. See text for further details.

far as we can proceed with the local calibration at present. Its status is clearly preliminary because of both the small number of galaxies and the extrapolation required, although in § VI, we note the consistency of slope of the local calibration with the cluster results.

V. INFRARED PHOTOMETRY COMPARED WITH OPTICAL MAGNITUDES

For the Virgo and Ursa Major galaxies, a direct comparison of the infrared with blue-magnitude/velocity-width relations is made in Figure 2. In Figure 2*a*, $H_{-0.5}$ is plotted against log $\Delta V(0)$ for our sample of Virgo galaxies (Table 1) which overlap with both ST and TF. For the same sample, in Figure 2*b* we have plotted $m_{pg}(0)$ values (i.e., Holmberg's 1958 total magnitudes corrected to face-on orientation) from TF against log $\Delta V(0)$, and in Figure 2*c* we have plotted $m_{pg}(0)$ values from ST against log $\Delta V(0)$. The log $\Delta V(0)$ values in Figures 2*a*–2*b* are from TF, while in Figure 2*c* they are from ST.

Holmberg magnitudes are not available for the Ursa Major galaxies. However, magnitudes on the B_T system from RC2 exist for a number of these objects. In Figure 2*d* we have plotted $H_{-0.5}$ against log $\Delta V(0)$ for those Ursa Major galaxies that have B_T's. With axial ratios from RC2, we corrected the B_T values to face-on orientation by employing both the inclination correction used by TF [$B_T^1(0)$] and that used by ST [$B_T^2(0)$]. These are plotted against log $\Delta V(0)$ in Figures 2*e* and 2*f*. All the log $\Delta V(0)$ values in Figures 2*d*–2*f* are from TF.

Least-squares solutions have been fitted to the data in Figure 2 and are shown there. In Table 5 we summarize several measurements of the correlation between the various quantities. A number of interesting results are apparent in Figure 2 and Table 5. First, *the correlation between $H_{-0.5}$ and log $\Delta V(0)$ is improved significantly over that for the optical magnitudes.*

Second, the inclination correction of ST for total internal absorption leads to a poorer correlation than the simpler correction procedure used by TF. Sandage and Tammann proposed that the scatter at the bright end of the magnitude/velocity-width relation is real and large. We believe Figure 2 does not support this conclusion, but rather, that it suggests the scatter seen by ST at the bright end is an artifact of the inclination corrections.

Finally, the slope of the correlation between $H_{-0.5}$ and log $\Delta V(0)$ suggested in Figures 1*a* and 1*d* is much steeper than the slope of the correlations from the optical magnitudes. That this result is primarily due to the infrared wavelength and not just an aperture effect is readily demonstrated. If, for instance, we correct the 12 points in Figure 2*e* from B_T to $B_{-0.5}$ by using the *B* growth curves in RC2, the slope of the ensuing least-squares line increases from -7.27 to -7.87, as compared to a slope of -9.46 in Figure 2*d*.

In the light of this discussion an interesting question arises concerning the optimal isophotal aperture size to be employed. Since the velocity $\Delta V(0)$ roughly measures $2V_{\max}$, which is in turn determined by the mass interior to the radius $r_{\max}$, the ideal aperture would clearly be at $r_{\max}$. Now the isophotal aperture corresponding to $r_{\max}$ varies with galaxy type, but for spirals we expect it to lie within the interval (-0.3, $+0.3$) in log A/D_0 (see Huchtmeier 1975). Additional scatter will be introduced into the magnitude/velocity-width relation depending on how much $L_A/L_{2r_{\max}}$ varies over the galaxy sample involved. Total *B* magnitudes will be badly affected by such dispersion both because of the large isophotal aperture ($\sim +0.6$ for B_T's and $+0.4$ for $m_{pg}(0)$ [see RC2]) and because of the different *B* growth curves for different morphological types. *H* magnitudes at log $A/D_0 = -0.5$, on the other hand, may be more appropriate to the problem.

VI. THE $H_{-0.5}$–LOG $\Delta V(0)$ RELATION FOR THE LOCAL CALIBRATORS, VIRGO, AND URSA MAJOR

In TF two morphological criteria were loosely employed to restrict the sample to (*a*) galaxies more edge-on than 45°, but less than 85°; and (*b*) galaxies of types Sb$^+$–Sc$^+$ in the Holmberg (1958) system. As discussed above, ST did not follow the first of these criteria. The second one was not strictly followed by either pair of authors. In particular, of the 10 Local Calibrators used by ST and TF, three are of type Im. For our own analysis, we have adhered to the first of these criteria but have ignored the second. In § VII

TABLE 5

COMPARISON OF VARIOUS CORRELATIONS

	x	y	N	$\|r\|$	$s_{y/x}$	$s_{x/y}$
Virgo	log $\Delta V(0)$ from TF	$H_{-0.5}$	8	0.97	0.30	0.027
	log $\Delta V(0)$ from TF	$m_{pg}(0)$ from TF	8	0.89	0.38	0.054
	log $\Delta V(0)$ from ST	$m_{pg}(0)$ from ST	8	0.86	0.53	0.073
UMa	log $\Delta V(0)$ from TF	$H_{-0.5}$	12	0.94	0.32	0.036
	log $\Delta V(0)$ from TF	$B_T^1(0)$	12	0.90	0.31	0.045
	log $\Delta V(0)$ from TF	$B_T^2(0)$	12	0.70	0.48	0.073

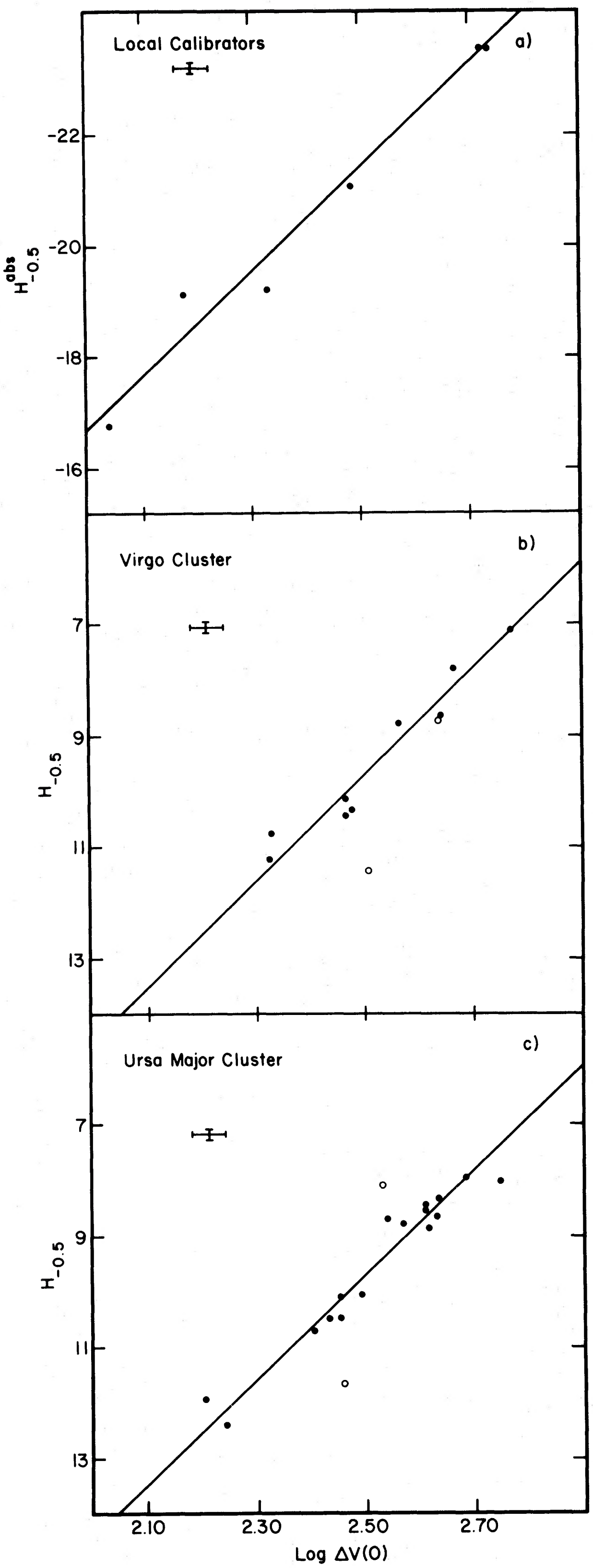

we show that any scatter introduced by morphological-type differences is likely to be minimized by using H magnitudes.

In Figure 3 we have plotted $H_{-0.5}$ against log $\Delta V(0)$ for the Local Calibrators, Virgo, and Ursa Major by using the data in Tables 1–4. $H_{-0.5}$ values were transformed to $H_{-0.5}{}^{\text{abs}}$ by using the distance moduli given in ST, adjusted again to a revised Hyades modulus of 3.23. The adjusted distances and $H_{-0.5}{}^{\text{abs}}$ values are listed in Tables 3 and 4. (Except for M31, TF used the same distances as ST.)

The calculated least-squares solutions shown in Figure 3 have been summarized in Table 6. The coefficients $a_\perp$ and $b_\perp$ in Table 6 were found by minimizing the *weighted perpendicular distance* of the points to the line. This solution is obtained by minimizing the quantity $\sum_i (y_i - a - bx_i)^2/(b^2\sigma^2_{x_i} + \sigma^2_{y_i})$. For the calculations in Table 6, we adopted an error of 0.03 for σ_x and 0.1 mag for σ_y. Because of both the large degree of correlation in the points and the steepness of the slope, these solutions are nearly identical to those obtained from minimizing the *unweighted* perpendicular distance. In fact, for the same reasons, the solutions obtained are almost independent of any reasonable variation in the weighting of the points.

While the agreement of the slope of the [$H_{-0.5}$, log $\Delta V(0)$]-relations in Figures 3*a*–3*c* may be partly fortuitous, it is still quite remarkable. The results in Table 6 suggest that the [$H_{-0.5}$, log $\Delta V(0)$]-correlation *is a universal relationship*. Furthermore, as discussed in § V, the slope of ~9.5 is significantly steeper than the slope of the relationship between optical magnitudes and H I velocity width, which was found by both TF and ST to range between 6 and 7.[2]

Also given in Table 6 are solutions obtained with the values of $\Delta V(0)$ preferred by ST. For the Local Calibrators, these values are close to those used by TF, and the solution is similar. The ST solution for Virgo, however, shows more scatter than the TF solution and has a significantly different slope. This change in slope is almost entirely due to the velocity width ST use for one galaxy, NGC 4651. In a detailed discussion of $\Delta V(0)$ values for all Virgo galaxies used by ST, Fisher and Tully (1977) concluded that the inclination angle for NGC 4651 is 59°, based on the opening of the spiral arms. This compares with 48° from ST and leads to a $\Delta V(0)$ difference of 78 km s^{-1}. Differences for the remaining galaxies are all less than 35 km s^{-1}. For the present purposes, we accept the $\Delta V(0)$ values of Fisher and Tully and believe that the first Virgo solution in Table 6 is to be preferred over the second one.

[2] A strict fitting procedure is unfortunately not applied by TF. Our own fit to their [$m_{pg}(0)$, log $\Delta V(0)$] Virgo relation (e.g., Fig. 2*b* here) leads to a slope of 7.5, rather than the value 6.25 quoted in TF from a fit by eye.

FIG. 3.—$H_{-0.5}$ magnitudes from Tables 1–4 are plotted against log $\Delta V(0)$ values from TF. The least-squares solutions shown have been fitted only to the filled circles.

TABLE 6

SOLUTIONS TO THE EQUATION $H^{-}_{0.5} = a + b[\log \Delta V(0) - 2.5]$

Sample	Source of $\Delta V(0)$*	Source of Distances*	N	$a_{\perp}$	$\sigma_{a,y/x}$	$b_{\perp}$	$\sigma_{b,y/x}$	$\|r\|$	$s_{y/x}$	$s_{x/y}$	$\chi^2_{\nu,y/x}$
Local	TF	ST	6	-21.35	0.40	- 9.47	0.16	0.99	0.47	0.051	20.7
Virgo	TF	—	9	9.72	0.62	- 9.67	0.24	0.97	0.37	0.039	12.5
Ursa Major	TF	—	16	9.73	0.45	- 9.36	0.18	0.97	0.33	0.037	10.3
Local	ST	ST	6	-21.30	0.40	- 9.52	0.16	0.99	0.48	0.051	21.0
Virgo	ST†	—	9	9.81	0.57	- 8.89	0.22	0.96	0.44	0.051	18.0
Local	TF	D	6	-20.81	0.40	-10.86	0.16	0.99	0.54	0.050	26.3

*TF - Tully and Fisher (1977).
ST - Sandage and Tammann (1976*b*).
D - de Vaucouleurs (1978*a*,*b*).

†TF values used for NGC 4498 and NGC 4758, which are not in ST.

We have also calculated a solution based on the distances to the Local Calibrators recently determined by de Vaucouleurs (1978*a*, *b*). The results are given in the last line of Table 6. The slope of this relation $|b| \sim 10.9$ is significantly steeper than the value of $|b| \sim 9.5$ obtained from the ST distances. If, in fact, the value 9.5 represents a universal relationship, then the (much closer) distances of de Vaucouleurs must be questioned.

Three galaxies in Virgo and two in Ursa Major are of particular interest, and we discuss each of them in turn.

NGC 4532 was rejected by Fisher and Tully (1977) from the Virgo sample because of the presence of a low-intensity profile wing. While NGC 4532 is included in our own solution for Virgo, we note that any correction for the effect of this wing would be in the sense of decreasing the profile width, which in turn would move the point for NGC 4532 closer to the regression line shown in Figure 2*b*. In fact, if the galaxy is excluded completely, our solutions for the intercept and slope become 9.66 and -9.40, respectively.

NGC 4535 has an inclination angle $<45°$ and was not included in the regressions.

IC 769 was detected marginally by TF at the rather large velocity of 2200 km s^{-1}. If this object is a background galaxy whose velocity is indicative of its true distance, we would expect it to lie ~ 1.5 mag below the mean Virgo relation. In fact, the galaxy lies ~ 1.8 mag below this mean relation. We take the view that IC 769 is a background object (as do Sandage and Tammann 1976*a*) and have excluded it from the regressions.

NGC 3556 has been noted by TF as being close to the Ursa Major cluster limit both spatially and in velocity, and they have suggested that it is a foreground galaxy. Our own observations of this object are complicated by the presence of a bright, superposed star in the beam. Our large infrared aperture did not permit separation of the star from the galaxy and accurate identification of the true nuclear location. For these reasons, we rejected NGC 3556 from the regression in Table 6.

UGC 6983 has an inclination $<45°$ and was rejected from our regressions.

VII. THE SLOPE OF THE RELATION AND ITS PHYSICAL BASIS

In addition to the tighter correlation, the increase in the slope of the $[H_{-0.5}, \log \Delta V(0)]$-relation over the blue relation is of considerable significance. The slope of the infrared relation is ~ 9.5, compared with the somewhat lesser values of 6–7 from TF and ST. The infrared slope is sufficiently close to 10 to be approximated by an $L_H \propto V_{\max}{}^4$ power law for physical purposes. Such a law is reminiscent of the $L_B \propto V_\sigma{}^4$ power law which approximates the luminosity/velocity-dispersion relation for ellipticals (Faber and Jackson 1976). That this resemblance is physically significant rather than a coincidence is demonstrated in this section. We begin with a naive treatment and then consider the general case.

For ellipticals, the quoted power law can be obtained from the empirical potential-energy law due to Fish (1964), $\Omega \propto M^{3/2}$. Then from the virial theorem,

$$Mv_\sigma{}^2 \propto M^{3/2}\,. \tag{1}$$

This results in the fourth-power law, given the assumption of constant *M/L between* galaxies (an assumption on which Fish's law itself depends). The constancy of M/L for ellipticals has been asserted by Sargent *et al.* (1977) from a similar argument and also by Schechter and Gunn (1979), although Faber and Jackson (1976) claimed a luminosity dependence.

In the case of spirals, since the bulge-to-disk ratio is probably a variable in addition to total mass, we consider two cases. In the first case we take the zero-thickness exponential disk rotating in its own potential field (Freeman 1970). The surface density distribution

$$\mu(r) = \mu_0 e^{-\alpha r} \tag{2}$$

is implied by the surface-brightness distribution and constant M/L. From the dimensionless rotation curve given by Freeman, we have

$$V_{\max} \approx 0.6(GM\alpha)^{1/2}, \tag{3}$$

which, when combined with the normalization of equation (2),

$$M = 2\pi\mu_0\alpha^{-2}, \tag{4}$$

yields

$$V_{\max}{}^4 \propto \mu_0 M. \tag{5}$$

Freeman's (1970) study of spirals has shown the remarkable constancy of μ_0 in the majority of cases. (A number of quite radical exceptions with different blue central surface brightness should not be ignored, however [Freeman 1970; Kormendy 1977].) A fourth-power law follows from equation (5), again with the assumption of constant M/L between galaxies of this type.

In the second case we consider a disk whose dynamics are dominated by a massive spheroidal component. For centrifugal equilibrium, we have

$$V_r^2 = GM_r/r, \tag{6}$$

where M_r is the mass within radius r. Assuming for simplicity a rotation curve which rises linearly to $V_{\max}$, we obtain

$$MV_{\max}{}^2 \propto \Omega \tag{7}$$

by integrating with respect to M_r, provided we assume a constant fraction of the total mass to be contained within the rising part of the rotation curve. The fourth-power law is obtained again by applying Fish's law to the assumed massive spheroidal component.

More generally, the basis of an $L \propto V^4$ power law can be found in the virial theorem and three assumptions. These are that (*a*) all galaxies have the same mass profiles and rotation curves as a function of some dimensionless scale-length, (*b*) all galaxies have the same central mass surface density, and (*c*) all galaxies have the same mean M/L. The details of this derivation are given in the Appendix.

Given the generality of this demonstration, why is an $L \propto V^4$ law seen in the infrared but not in the blue? We propose a simple answer, that in the latter case assumption (*c*) is invalid. *We suggest that M/L_B is not constant in spirals of differing mass, but that M/L_H is constant.* This is highly plausible, as L_B primarily measures the contribution of the active Population I component, whereas L_H mainly measures the old population of red giants (see below). A lower mass-to-light ratio in the blue (more blue light per unit mass) might be expected with advancing morphological type and decreasing luminosity. This would act to make the power-law relationship considerably shallower, as is observed. A dependence $M/L_B \sim L_H{}^{1/4}$ is suggested.

Three pieces of separate evidence support the proposition that a massive old population is measured by $H_{-0.5}$ in spirals. First, the integrated 2.0 μm H_2O index, 2.4 μm CO index, and broad-band infrared colors for spirals *of nearly all types* are comparable to those observed in ellipticals (Paper V), which suggests that the infrared light is dominated by late-type giants (Frogel *et al.* 1978; Aaronson, Frogel, and Persson 1978), but not by supergiants. Second, the $V - K$ colors of blue irregular galaxies indicate that even in these objects only 0.02–0.04 of the total mass has undergone recent star formation (see Aaronson 1978; Struck-Marcell and Tinsley 1978). Third, the H magnitude growth curves for spirals (Fig. 1) are shallower than in the blue and resemble those of ellipticals rather closely. The mean infrared growth curve for the latter (Frogel *et al.* 1978) has slope 2.1 for the interval (−0.6, −1.0) in log $A/D(0)$. The slopes of the growth curves in Figure 1 evaluated in the same interval are 2.0 for types S0/a–Sab, 2.1 for types Sb–Sbc, and 2.6 for types Sc–Sd. By comparison, the corresponding blue slopes from RC2 are 2.1, 2.3, 2.9, and 3.35. These results can be understood as the composite effect of a young population with a blue radial gradient superposed on an old red population which is perhaps more spherically distributed.

This, we suggest, is the key to the success of the infrared magnitude/velocity-width relation: that we see predominantly the old population common to all late-type galaxies, unadulterated by the absorption (dust) and emission (blue stars) of the young population.

VIII. APPLICATION TO THE DISTANCE SCALE

In this section we estimate the distance moduli to Virgo and Ursa Major and consider the implied value of the Hubble constant. *We stress that because of the provisional nature of the Local calibration these results should be considered as preliminary.*

a) Distance Moduli to Virgo and Ursa Major

Given the similarity in slopes for the [$H_{-0.5}$, log $\Delta V(0)$]-relations in Table 6, an estimate of the distance moduli can be found simply by differencing the intercepts for Virgo and Ursa Major with the intercept for the Local Calibrators solution. The result obtained is 31.07 ± 0.25 mag for Virgo and 31.08 ± 0.19 mag for Ursa Major, the errors being in the formal sense only.

Alternatively, we can use the solution for the Local Calibrators to calculate individually the distance modulus for each galaxy in either Virgo or Ursa Major, and then take the mean (the procedure followed by ST). The moduli obtained are the same as in the intercept method, with slightly smaller formal errors. For comparison, we have applied this procedure with the ST $\Delta V(0)$ values and also with the distances to the Local Calibrators from de Vaucouleurs 1978*a*, *b*). Our results for all four approaches are summarized in Table 7.

TABLE 7

SEVERAL ESTIMATES OF THE DISTANCE SCALE AND THE EXPANSION RATE

Method	Source of Local Cal. Distances	Source of $\Delta V(0)$	Virgo $H_{-0.5} - H^{abs}_{-0.5}$ (mag)	Virgo H_0 (km s^{-1} Mpc^{-1})	UMa $H_{-0.5} - H^{abs}_{-0.5}$ (mag)	UMa H_0 (km s^{-1} Mpc^{-1})
Difference in intercepts	ST	TF	31.07 ±0.25	67 ±8	31.08 ±0.19	58 ±5
Individual moduli	ST	TF	31.07 ±0.20	67 ±7	31.08 ±0.16	58 ±4
Individual moduli	ST	ST + TF*	31.14 ±0.20	65 ±7	31.03 ±0.16	59 ±4
Individual moduli	D	TF	30.56 ±0.21	85 ±8	30.57 ±0.16	73 ±5

*ST used for Local Calibrators and Virgo, except for NGC 4498 and NGC 4758.
TF used for NGC 4498 and NGC 4758 and for Ursa Major.

b) *The Hubble Constant*

If the mean recessional velocities of the Virgo and Ursa Major clusters are not perturbed relative to the Hubble flow, a value for the Hubble constant H_0 can be determined from their distance moduli. In regard to Virgo, Peebles (1978) has summarized the evidence for a rather small correction for such a departure (~ 30 km s^{-1}), based on the relative moduli of Virgo and Coma. Neglecting any correction, we adopt 1100 ± 68 km s^{-1} (ST) and 949 ± 19 km s^{-1} (TF) for the cosmological redshifts of Virgo and Ursa Major, respectively.

For the different moduli obtained above, Table 7 gives the consequent values of H_0. Note that the formal errors in these determinations are weighted heavily by uncertainties in the Local calibration (e.g., Table 6, lines 1, 4, and 6) and, for Virgo, by the uncertainty in the mean recessional velocity. Only those values obtained by using the de Vaucouleurs (1978*a*, *b*) distance scale are significantly different from 60 km s^{-1} Mpc^{-1}. Evidence has already been quoted for the inconsistency of the Local Calibrators relation found by using this distance scale with the relations obtained in Virgo and Ursa Major. Although we do not regard this evidence as conclusive, we think it reasonable to prefer the ST distance scale at present, and so obtain a mean value of $H_0 = 61 \pm 4$ km s^{-1} Mpc^{-1}. We note that the fair agreement between the values of H_0 obtained from either Virgo or Ursa Major lends credence to the assumption that the mean velocities of these clusters are not *significantly* perturbed relative to the Hubble flow.

Our preliminary value of $H_0 = 61 \pm 4$ km s^{-1} Mpc^{-1} lies between the value of 70 ± 8 km s^{-1} Mpc^{-1} from the revised analysis of Fisher and Tully (1977) and that of 53 ± 6 km s^{-1} Mpc^{-1} from ST. Further discussion must clearly await improvement of our Local calibration, along the lines outlined in the next section.

IX. SUMMARY

The infrared luminosity/H I velocity-width relation has emerged as a superior expression of the original Tully-Fisher relation obtained in the blue for two important reasons:

1. A tighter empirical correlation has been found in the Virgo and Ursa Major clusters by using H magnitudes uncorrected for inclination rather than by using blue or photographic magnitudes with their individually uncertain, prescribed corrections for internal (and galactic) absorptions. In the [$H_{-0.5}$, $\log \Delta V(0)$]-relations the H magnitudes are simply obtained from multiaperture measurements interpolated or extrapolated to $\log A/D(0) = -0.5$, and the observed velocity widths (following Tully and Fisher) are corrected for inclination to an edge-on value. Other corrections to the magnitudes have been shown to be negligible.

2. The true form of the relationship has emerged as an $L \propto V^4$ power law. Since it is fundamentally a dynamical law ($M \propto V_{\max}{}^4$), the Tully-Fisher relation requires a wavelength where luminosity is most directly related to total mass to appear in the above form. Because this form is achieved at 1.6 μm, we have suggested that M/L_H is generally constant for late-type galaxies, whereas the mass-to-blue-light ratio is directly related to luminosity ($M/L_B \propto L_H{}^{1/4}$), probably due to more active star formation in galaxies of later type and lower luminosity. A comparison of growth curves suggests that the mass seen at H may be more spherically distributed than the blue light. Further investigation of this point from 1.6 μm surface photometry would be very valuable.

We have proceeded to apply the new infrared relation to the distance scale. These results must be considered preliminary because (*a*) the sample of Local Calibrators is incomplete and (*b*) for three galaxies significant growth-curve extrapolation was required to reach $\log (A/D_0) = -0.5$. With the Sandage and

Tammann distances to nearby galaxies, the respective distance moduli obtained for Virgo and Ursa Major are 31.07 ± 0.20 and 31.08 ± 0.16, which lead to a combined value for H_0 of 61 ± 4 km s^{-1} Mpc^{-1}. This value lies between those of TF and ST. The similarity of the $[H_{-0.5}, \log \Delta V(0)]$-correlation for the Local Calibrators, Virgo, and Ursa Major, combined with what we believe is a sound physical explanation for this correlation, suggest that the slope of the relationship is universal in nature.

We expect that work currently in progress with very small telescopes will both extend the Local Calibration, especially in regard to the M81 and Sculptor groups, and minimize the need for extrapolation. We would add that the formal errors quoted above should not be considered definitive, first, because of the preliminary nature of the calibration, but also because of uncertainties in the *distances* to the Calibrators. For instance, it is difficult to accept that the Hyades is the weakest link in the chain of distance determinations within the Local Group, and yet a recent shift in this distance alone was responsible for a 10% change in H_0. Further study of the distances to nearby galaxies is an urgent requirement if good use is to be made of the refined tool that infrared photometry has developed from the Tully-Fisher distance method. Ongoing measurements of H magnitudes and velocity widths both for galaxies in more distant clusters and for galaxies in the general field should help in understanding the local velocity field by providing a better calibration of the Hubble constant and improved determinations of galaxy peculiar motions.

It is a pleasure to thank Paul Schechter for a number of enlightening conversations. This work was partially supported with funds from NSF grants AST 76-81874 and AST 76-22991.

APPENDIX

THE DYNAMICAL BASIS OF AN $L \sim V^4$ POWER LAW

Consider a set of galaxies with density distributions of the form

$$\rho(\boldsymbol{r}) = \rho_0 f(\boldsymbol{r}/r_e) = \rho_0 f(\boldsymbol{x}) . \tag{8}$$

The corresponding surface density distribution on the plane of the sky is

$$\mu(\boldsymbol{r}) = \mu_0 g(\boldsymbol{r}/r_e) = \mu_0 g(\boldsymbol{x}) , \tag{9}$$

where the functions f and g are dimensionless relations, and r_e is a scale length. The function $\mu(\boldsymbol{r})$ is exemplified by the Hubble or de Vaucouleurs law.

We assume that the rotation curve may similarly be written

$$V(\boldsymbol{r}) = V_m h(\boldsymbol{x}) , \tag{10}$$

and calculate the kinetic and potential energies as follows:

$$T = \tfrac{1}{2}\int \rho(\boldsymbol{r}) V^2(\boldsymbol{r}) d\tau = \tfrac{1}{2}\rho_0 V_m{}^2 r_e{}^3 \int f(\boldsymbol{x}) h^2(\boldsymbol{x}) d\tau = \tfrac{1}{2}\rho_0 V_m{}^2 r_e{}^3 a , \tag{11}$$

where a is a numerical constant obtained from the dimensionless integral

$$\Omega = \tfrac{1}{2}\int \Phi(\boldsymbol{r})\rho(\boldsymbol{r}) d\tau , \tag{12}$$

where $\Phi(\boldsymbol{r})$ is the gravitational potential at $\boldsymbol{r}$. This can be written using the Green's function solution of Poisson's equation,

$$\Omega = \tfrac{1}{2}G\rho_0{}^2 \int f(\boldsymbol{r}) \int \frac{f(\boldsymbol{r}')}{|\boldsymbol{r} - \boldsymbol{r}'|} d\tau' d\tau = \tfrac{1}{2}G\rho_0{}^2 r_e{}^5 \iint \frac{f(\boldsymbol{x}')}{|\boldsymbol{x} - \boldsymbol{x}'|} d\hat{\tau}' d\hat{\tau} = \tfrac{1}{2}G\rho_0{}^2 r_e{}^5 b . \tag{13}$$

In (13), $d\hat{\tau}$ is a dimensionless volume element and b is the dimensionless integral.

From the virial theorem,

$$V_m{}^2 = \tfrac{1}{2}G\rho_0 r_e{}^2 b/a . \tag{14}$$

By integration of (8) and (9),

$$M = \mu_0 r_e{}^2 \int g(\boldsymbol{x}) d\hat{\sigma} = \mu_0 r_e{}^2 c = \rho_0 r_e{}^3 \int f(\boldsymbol{x}) d\hat{\tau} = \rho_0 r_e{}^3 d , \tag{15}$$

we finally obtain

$$V_m{}^4 = \frac{b^2 c}{4a^2 d^2} \mu_0 G^2 M . \tag{16}$$

The power law follows from the assumptions of constancy of μ_0 and M/L.

We are grateful to Paul Schechter for first demonstrating to us a relation of this form.

REFERENCES

Aaronson, M. 1978, *Ap. J.* (*Letters*), **221**, L103.
———. 1979, in preparation (Paper V).
Aaronson, M., Frogel, J. A., and Persson, S. E. 1978, *Ap. J.*, **220**, 442.
de Vaucouleurs, G. 1978*a*, *Ap. J.*, **223**, 730.
———. 1978*b*, *Ap. J.*, **224**, 710.
de Vaucouleurs, G., and de Vaucouleurs, A. 1964, *Reference Catalogue of Bright Galaxies* (Austin: University of Texas Press).
de Vaucouleurs, G., de Vaucouleurs, A., and Corwin, H. G. 1976, *Second Reference Catalogue of Bright Galaxies* (Austin: University of Texas Press) (RC2).
Faber, S. M., and Jackson, R. E. 1976, *Ap. J.*, **204**, 668.
Fish, R. 1964, *Ap. J.*, **139**, 284.
Fisher, J. R., and Tully, R. B. 1977, *Comm. Ap.*, **7**, 85.
Freeman, K. C. 1970, *Ap. J.*, **160**, 811.
Frogel, J. A., Persson, S. E., Aaronson, M., and Matthews, K. 1978, *Ap. J.*, **220**, 75.
Hanson, R. B. 1975, *A.J.*, **80**, 379.
Holmberg, E. 1958, *Medd. Lunds Obs.*, Ser. 2, No. 136.
Huchtmeier, W. K. 1975, *Astr. Ap.*, **45**, 259.
Huchtmeier, W. K., Tammann, G. A., and Wendker, H. J. 1976, *Astr. Ap.*, **46**, 381.
Johnson, H. L. 1968, in *Stars and Stellar Systems*, Vol. **7**, ed. B. M. Middlehurst and L. H. Aller (Chicago: University of Chicago Press), p. 167.
Kormendy, J. 1977, *Ap. J.*, **217**, 406.
Nilson, P. N. 1973, *Uppsala General Catalogue of Galaxies*, *Uppsala Obs. Ann.*, Vol. **6** (UGC).
Peebles, P. J. E. 1978, talk presented at AAS meeting, Austin Texas.
Sandage, A. 1961, *The Hubble Atlas of Galaxies* (Washington: Carnegie Institution, Pub. No. 618).
Sandage, A., and Tammann, G. A. 1976*a*, *Ap. J.* (*Letters*), **207**, L1.
———. 1976*b*, *Ap. J.*, **210**, 7 (ST).
Sargent, W. L. W., Schechter, P. L., Boksenberg, A., and Shortridge, K. 1977, *Ap. J.*, **212**, 326.
Schechter, P. L., and Gunn, J. E. 1979, in preparation.
Struck-Marcell, C., and Tinsley, B. M. 1978, *Ap. J.*, **221**, 562.
Tully, R. B., and Fisher, J. R. 1976, in *Proceedings IAU Colloquium No. 37, Décalages vers le Rouge et Expansion de l'Univers* (Paris: C.N.R.S.), p. 95.
———. 1977, *Astr. Ap.*, **54**, 661 (TF).
van den Bergh, S. 1976, in *Proceedings IAU Colloquium No. 37, Décalages vers le Rouge et Expansion de l'Univers* (Paris: C.N.R.S.), p. 13.

MARC AARONSON: Steward Observatory, University of Arizona, Tucson, AZ 85721

JOHN HUCHRA: Center for Astrophysics, 60 Garden Street, Cambridge, MA 02138

JEREMY MOULD: Hale Observatories, 813 Santa Barbara Street, Pasadena, CA 91101